Knee Surg Sports Traumatol Arthrosc
DOI 10.1007/s00167-010-1372-1

KNEE

Radiographic landmarks for tunnel positioning in double-bundle ACL reconstructions

Sean D. Pietrini · Connor G. Ziegler · Colin J. Anderson · Coen A. Wijdicks · Benjamin D. Westerhaus · Steinar Johansen · Lars Engebretsen · Robert F. LaPrade

Received: 3 August 2010 / Accepted: 13 December 2010

Abstract
Purpose The purpose of this study was to establish quantitative and qualitative radiographic landmarks for identifying the femoral and tibial attachment sites of the AM and PL bundles of the native ACL and to assess the reproducibility of identification of these landmarks using intraclass correlation coefficients. It was hypothesized that the radiographic positions of the AM and PL bundles could be defined in relation to anatomic landmarks and radiographic reference lines.
Methods The femoral and tibial attachment sites of the AM and PL bundles on twelve cadaveric knees were labeled with radio-opaque markers. The positions of the AM and PL bundle attachment sites were quantified on radiographs by three independent examiners.
Results On the lateral femoral view, the AM bundle was located at 21.6 ± 5.6% of the sagittal diameter of the femur drawn along Blumensaat's line and 14.2 ± 7.7% distal to the notch roof along the maximum notch height. The PL bundle was located at 28.9 ± 4.6% of the sagittal diameter and 42.3 ± 6.0% of the notch height. The knee flexion angle at which the AM and PL bundle attachment sites were horizontally oriented was 115 ± 7.1°. On the tibial AP view, the AM and PL bundles were located at 44.2 ± 3.4 and 50.1 ± 2.1%, respectively, from the medial aspect of the tibia along its coronal diameter. On the lateral view, the distances from the AM and PL bundles to the anterior tibial margin measured along the tibial sagittal diameter were 36.3 ± 3.8 and 51.0 ± 4.0%, respectively. The center of the PL bundle attachment was located almost precisely at the center of the tibial plateau in both the coronal and sagittal planes.
Conclusions This study defines the radiographic locations of the femoral and tibial bundle attachment sites of the native ACL and a reliable and transferrable protocol for identifying these sites on radiographs in relation to surrounding landmarks and digitally projected reference lines. In addition, it was found that the femoral attachments of the AM and PL bundles were horizontally aligned at 115° of knee flexion and the PL bundle tibial attachment was located essentially at the center of the tibia.

Clinical relevance These radiographic guidelines can facilitate more accurate tunnel placement in double-bundle ACL reconstructions incorporating intra-operative fluoroscopic techniques, and also enhance pre-operative planning and post-operative evaluations of these procedures.

S. D. Pietrini · C. G. Ziegler · C. J. Anderson · B. D. Westerhaus
Orthopaedic Biomechanics Lab,
Department of Orthopaedic Surgery,
University of Minnesota, Minneapolis, MN, USA

C. A. Wijdicks · R. F. LaPrade (✉)
Steadman Philippon Research Institute,
181 W. Meadow Drive, Suite 1000,
Vail, CO 81657, USA
e-mail: drlaprade@sprivail.org

S. Johansen · L. Engebretsen
University Hospital and Faculty of Medicine,
Orthopaedic Center, University of Oslo, Oslo, Norway

Keywords Double-bundle ACL reconstructions · Tunnel placement · Radiographic guidelines · Anteromedial bundle · Posterolateral bundle

Introduction

Attempts at improving clinical outcomes for patients undergoing single-graft, single-bundle reconstructions of

Published online: 11 January 2011

the anterior cruciate ligament (ACL) have included the development of double-bundle reconstruction techniques that separately reconstruct the functionally distinct anteromedial (AM) and posterolateral (PL) bundles of the ACL (Fig. 1) [1, 4, 7–10, 13, 19, 21, 24, 25]. As double-bundle ACL reconstructions become more common, a comprehensive, clinically reproducible set of guidelines to assess the radiographic locations of the native ACL bundle attachment sites is needed. Radiographic guidelines for locating the ACL bundle attachment sites would facilitate more accurate tunnel placement during double-bundle reconstruction surgeries, and also aid in post-operative evaluations of these reconstructions and pre-operative planning of revision surgeries.

The purpose of this study was to establish quantitative and qualitative radiographic landmarks for identifying the femoral and tibial attachment sites of the AM and PL bundles of the native ACL and to assess the reproducibility of identification of these landmarks using intraclass correlation coefficients. It was hypothesized that a standardized protocol could be used to consistently and reproducibly describe the positions of the ACL bundle attachment sites in relation to bony and soft-tissue landmarks, as well as to reference lines projected onto radiographic images.

Materials and methods

Sample preparation

Twelve non-paired, fresh-frozen cadaveric knees (mean age 57.8; range 45–70) with no history of prior injury or osteoarthritis were utilized in this study. All tissue except the ACL, menisci, and collateral ligaments was removed. With the knees flexed to >90°, the ACL was carefully separated at its femoral attachment sites into the AM and PL bundles using a blunt-tipped probe. The alignment of the femoral bundle attachment sites was nearly horizontal at this position, and the distinct orientation and tensioning pattern of the fibers of each bundle could be more easily observed and separated compared to its tibial attachment orientation. Sutures were passed around the mid-substance of each bundle approximately 1 cm from both the femoral and tibial attachment sites, and the bundles were then excised midway between these sutures.

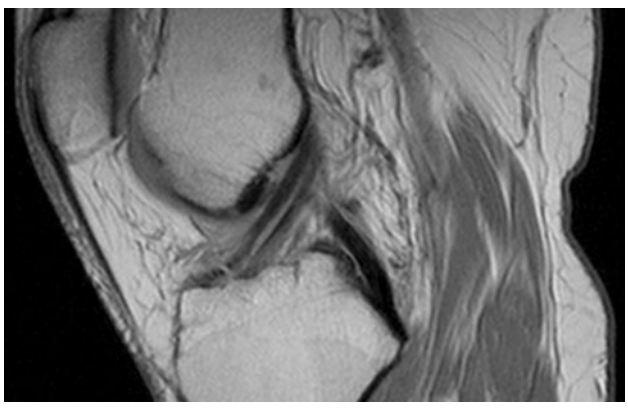

Fig. 1 Sagittal proton density turbo spin echo MRI demonstrating the parallel orientation of the anteromedial (*AM*) and posterolateral (*PL*) bundles of the ACL near full knee extension

Subsequently, the attachment centers were identified by tensioning the bundle remnants and observing the direction of the central fibers projecting onto the bony surface [5], and the peripheries were immediately marked with a permanent ink pen. The centers of the bundles were labeled with 2-mm stainless steel spheres (Small Parts Inc., Miami Lakes, Florida). The spheres were shallowly embedded in bone according to a previously described technique [14, 22].

After anteroposterior (AP) radiographs of the femur were acquired, the knees were disarticulated. On the femur, the bundle remnants were sharply dissected from bone, and the bundle attachment footprints were immediately marked with a radio-opaque barium sulfate ($BaSO_4$) emulsion in preparation for radiographic imaging in the lateral view.

Lateral radiographs of the tibia were obtained after the center, anterior edge, and posterior edge of each attachment footprint, as well as the anterior and posterior horns of the lateral meniscus and the retro-eminence ridge, were marked with 1-mm diameter T-pins (Advantus Corporation, Jacksonville, Florida). Pins were subsequently removed from the edges of the attachment footprints, the posterior horn of the lateral meniscus, and the retro-eminence ridge, and an additional pin was inserted at the anterior horn of the medial meniscus; following this adjustment in labeling, the tibia was imaged in the AP view. Finally, the tibial diaphysis was cut 2 cm distal and parallel to the articular cartilage surface using an oscillating saw. An axial radiograph of the proximal portion was then obtained after the tibial attachment footprints were labeled with $BaSO_4$ to allow for qualitative radiographic assessment of footprint morphology, and pins were placed at the posterior horn attachments of the lateral and medial menisci, the retro-eminence ridge, and the most anterior edge of the tibial plateau.

Image collection and measurements

A fluoroscopy C-arm (MiniView 6800 Mobile Imaging System, GE Healthcare, Milwaukee, Wisconsin) captured AP, lateral, and axial images of each specimen. True AP views were obtained with the anterior and posterior margins of the medial tibial plateau closely superimposed and

the intercondylar eminences of the tibia positioned at the center of the femoral intercondylar notch, according to previously described techniques [14, 22]. True lateral radiographs were obtained by ensuring that the posterior aspects of the medial and lateral femoral condyles overlapped. A 1 cm × 1 cm radio-opaque grid was included on all radiographs to correct for magnification disparities due to potential variability in distances between the specimens and the x-ray source.

Quantitative radiographic measurements were performed in a picture archiving and communication system (PACS) (Imagecast, IDX Systems Corporation, Buckinghamshire, United Kingdom). The positions of each bundle attachment were determined in relation to previously labeled landmarks and reference lines projected onto the radiographs in PACS.

Fluoroscopic imaging of the femur in the anterior–posterior (AP) view (Fig. 2a) was performed at 0°, 55° (the approximate angle of knee flexion at which the maximum height of the intercondylar notch was visible on the AP view), and 90° of knee flexion to evaluate the effect of intercondylar notch orientation on radiographic measurements. The locations of the bundle centers were quantified as percentages of the maximum height of the intercondylar notch (line H, for height), measured perpendicular to a line that intersected the distal aspects of the femoral condyles. The epicondylar width was also measured as a means of normalizing knee size among specimens and accounting for variability in the dimensions of the intercondylar notch.

Analysis of the femoral attachment locations of the AM and PL bundles on the lateral view was performed according to a previously described quadrant method with modified terminology (Fig. 2b) [3, 5, 26]. Four distances were measured: the sagittal diameter of the lateral femoral condyle along Blumensaat's line (line B, for Blumensaat), the maximum height of the notch drawn perpendicular to Blumensaat's line and extending to the most distal aspect of the femoral condyle (line H), the distances between the bundle centers and the most posterior subchondral contour of the lateral femoral condyle (running parallel to and expressed as a percentage of line B, and thus referred to as distance B_p), and the distances between the bundle centers and Blumensaat's line (running parallel to and expressed as a percentage of line H, and thus referred to as distance H_p). Perpendicular distances between the bundle centers and a line projected distally along the posterior femoral cortex (line PC, for posterior cortex) were also measured [14, 15, 22]. Finally, the knee flexion angle at which the femoral bundle attachments were oriented horizontally with respect to one other was calculated.

On AP radiographs of the tibia (Fig. 3a), a reference line intersecting the most proximal portions of the tibial plateau and spanning the maximum coronal (lateral–medial) diameter of the tibial surface (line CD, for coronal diameter) was used to calculate percentage-based measurements of the locations of the attachment centers in relation to the most medial aspect of the medial tibial plateau. Additional reference lines were drawn extending distally from the apexes of the lateral and medial intercondylar eminences (Fig. 3a), and the location of each tibial attachment center was quantified perpendicular to these lines.

On lateral radiographs of the tibia (Fig. 3b), the anterior–posterior positions of the attachment centers and edges of the AM and PL bundles were measured based on a previously described technique [2, 6]. According to this method, a line representing the maximum sagittal (anterior–posterior) diameter of the tibia (line SD, for sagittal diameter) was drawn parallel to the joint line from the most

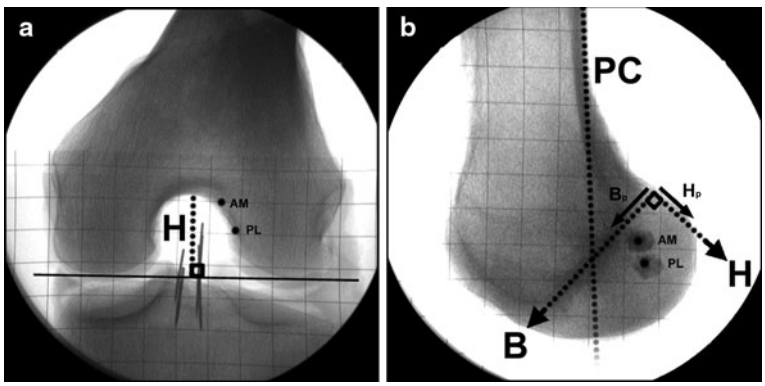

Fig. 2 AP (**a**) and lateral (**b**) knee radiographs of left femoral specimens, with ACL bundle footprints labeled with barium sulfate in the lateral view. *AM* center of the anteromedial bundle attachment, *PL* center of the posterolateral bundle attachment, *H* maximum height of the intercondylar notch drawn perpendicular to Blumensaat's line and extending to the most distal aspect of the femoral condyle, *B* maximum sagittal diameter of the lateral femoral condyle along Blumensaat's line, B_p anterior–posterior distance drawn from the bundle centers to the most dorsal subchondral contour and running parallel to line B/Blumensaat's line, H_p proximal–distal distance drawn from the bundle centers to Blumensaat's line and running parallel to line H, *PC* posterior femoral cortex extension line

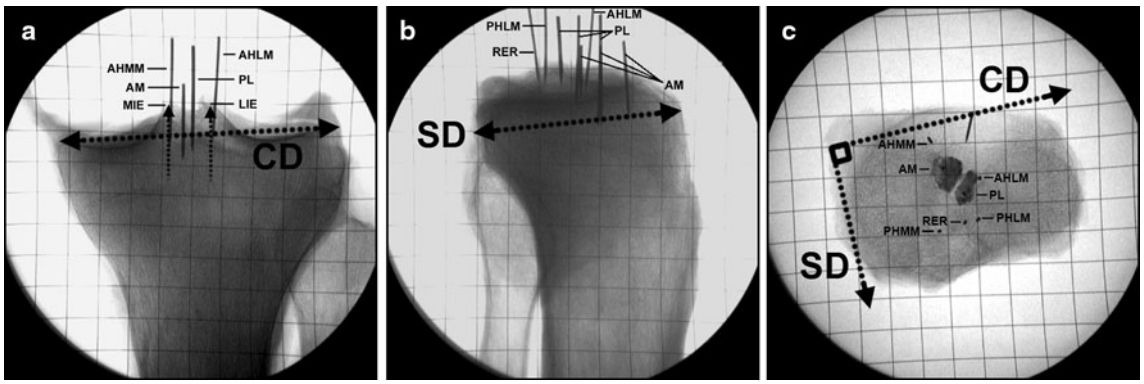

Fig. 3 AP (**a** left tibia), lateral (**b**), and axial (**c** right tibia) knee radiographs of the tibia, with ACL bundle footprints labeled with barium sulfate in the axial view. *AM* center of the anteromedial bundle attachment, *PL* center of the posterolateral bundle attachment, *LIE* lateral intercondylar eminence, *MIE* medial intercondylar eminence, *AHLM* anterior horn of the lateral meniscus, *AHMM* anterior horn of the medial meniscus, *PHLM* posterior horn of the lateral meniscus, *PHMM* posterior horn of the medial meniscus, *CD* maximum coronal diameter of the tibia plateau, *SD* maximum sagittal diameter of the tibial plateau

posterior corner of the proximal tibial plateau to the most anterior tibial margin (Fig. 3b). The locations of the attachment markers for each structure were measured as percentages of the total length of the sagittal diameter line calculated with respect to the anterior tibial margin.

Both the maximum coronal and sagittal diameters (lines CD and SD, respectively) of the tibia were projected onto axial radiographs and utilized for percentage-based, two-dimensional quantification of the AM and PL bundle attachments centers, the anterior and posterior horns of the lateral and medial menisci, and the retro-eminence ridge (i.e., the transverse ridge located at the apex of the posterior slope of the tibial plateau just anterosuperior to the tibial PCL attachment) (Fig. 3c).

Statistical analysis

To determine interobserver reliability, three examiners of differing experience levels *(blinded for review)* were assigned to independently generate the previously described reference lines and perform measurements on blinded radiographs using PACS. Each examiner measured the same set of blinded radiographs on two separate occasions at least 2 weeks apart to evaluate intraobserver reliability. Subsequently, single-measure intraclass correlation coefficients (ICCs) (SPSS Inc, Chicago, Illinois) were used to determine variability within and among measurement groups.

Results

The most clinically relevant, radiographic-based measurements are presented below, with the remainder included in Tables 1, 2, 3, 4, 5. All measurements were normalized according to the femoral epicondylar width. Measurements involving structures labeled with spheres were made in reference to the spherical centers, whereas those involving pinned structures were made at the points where the pins penetrated the subchondral bone. The locations of soft tissue landmarks on the tibia were also quantified and are reported in Tables 3, 4, 5.

Table 1 Quantitative relationships of the femoral attachments of the ACL bundles to landmarks and reference lines on anterior–posterior radiographs

Relationship	Distance
Proximal–distal distance between AM and PL bundle centers at:	
Full knee extension	8.6 ± 2.0 mm
55° of knee flexion	8.8 ± 1.9 mm
90° of knee flexion	5.6 ± 1.8 mm
Notch height percentage of AM bundle center at:	
55° of knee flexion	11.9 ± 2.2%
90° of knee flexion	18.4 ± 8.7%
Notch height percentage of PL bundle center at:	
55° of knee flexion	39.8 ± 6.7%
90° of knee flexion	39.1 ± 8.5%

Values reported as the mean and standard deviation. Notch height percentage refers to the distance from the given bundle center to the roof of the intercondylar notch quantified as a percentage of the maximum notch height (line H)

AM anteromedial, *PL* posterolateral

Femur

Anterior–posterior view

Radiographic measurements for the AP view of the femur are illustrated in Fig. 4a and reported quantitatively in Table 1. In full extension, the proximal–distal distance

Table 2 Quantitative relationships of the femoral attachments of the ACL bundles to landmarks and reference lines on lateral radiographs

Relationship	Distance
Distance between AM and PL bundle centers in the:	
Proximal–distal direction	9.6 ± 1.9 mm
Anterior–posterior direction	8.7 ± 3.6 mm
Percentage-based distance from AM bundle center:	
To line H (distance B_p)	21.6 ± 5.6%
To line B (distance H_p)	14.6 ± 7.7%
Percentage-based distance from PL bundle center:	
To line H (distance B_p)	28.9 ± 4.6%
To line B (distance H_p)	42.3 ± 6.0%
Distance from AM bundle center to posterior cortex extension line	11.6 ± 4.4 mm
Distance from PL bundle center to posterior cortex extension line	15.8 ± 4.3 mm
Knee flexion angle at which AM and PL bundle centers were oriented horizontally	115.0 ± 7.1°

Values reported as the mean and standard deviation. Line B represents the maximum sagittal diameter of the lateral femoral condyle along Blumensaat's line. Line H represents the maximum height of the intercondylar notch. Distance B_p refers to the position of the bundle center expressed as a percentage of line B. Distance H_p refers to the position of the bundle center expressed as a percentage of line H

AM anteromedial, *PL* posterolateral

Table 3 Quantitative relationships of tibial ACL bundle landmarks to reference lines on anterior–posterior radiographs

Relationship	Distance
Distance between AM and PL bundle centers along the coronal diameter line	5.7 ± 2.5 mm
Coronal percentage of:	
AM attachment	44.2 ± 3.4%
PL attachment	50.1 ± 2.1%
Anterior horn of lateral meniscus	59.0 ± 2.7%
Anterior horn of medial meniscus	35.1 ± 6.2%
Lateral intercondylar eminence	56.5 ± 3.0%
Medial intercondylar eminence	40.7 ± 3.5%

Values reported as the mean and standard deviation. Coronal percentage refers to the distance from the given landmark to the medial margin of the tibia measured as a percentage of the maximum coronal diameter of the tibia (line CD)

AM anteromedial, *PL* posterolateral

Table 4 Quantitative relationships of tibial ACL bundle landmarks to reference lines on lateral radiographs

Relationship	Distance
Distance between AM and PL bundle centers along the sagittal diameter line	8.7 ± 2.6 mm
Sagittal percentage of:	
Anterior edge of AM attachment	28.9 ± 3.3%
Center of AM attachment	36.3 ± 3.8%
Posterior edge of AM attachment	49.7 ± 5.2%
Anterior edge of PL attachment	41.2 ± 4.4%
Center of PL attachment	51.0 ± 4.0%
Posterior edge of PL attachment	59.3 ± 4.7%
Anterior horn of lateral meniscus	43.6 ± 4.2%
Posterior horn of lateral meniscus	64.2 ± 4.5%
Retro-eminence ridge	65.0 ± 4.2%

Values reported as the mean and standard deviation. Sagittal percentage refers to the distance from the given landmark to the anterior margin of the tibia measured as a percentage of the maximum sagittal diameter of the tibia (line SD)

AM anteromedial, *PL* posterolateral

Table 5 Quantitative relationships of tibial ACL bundle landmarks to reference lines on axial tibial radiographs

Relationship	Distance
Coronal percentage of:	
AM attachment	52.0 ± 3.0%
PL attachment	48.8 ± 2.7%
Anterior horn of lateral meniscus	41.0 ± 2.8%
Posterior horn of lateral meniscus	45.7 ± 3.8%
Anterior horn of medial meniscus	55.6 ± 5.5%
Posterior horn of medial meniscus	62.5 ± 3.3%
Sagittal percentage of:	
AM attachment	37.7 ± 6.6%
PL attachment	51.8 ± 4.6%
Anterior horn of lateral meniscus	46.2 ± 4.7%
Posterior horn of lateral meniscus	69.3 ± 5.5%
Anterior horn of medial meniscus	12.9 ± 5.9%
Posterior horn of medial meniscus	73.5 ± 7.4%
Retro-eminence ridge	72.1 ± 8.7%

Values reported as the mean and standard deviation. Coronal percentage refers to the distance from the given landmark to the lateral margin of the tibia measured as a percentage of the maximum coronal diameter of the tibia (line CD). Sagittal percentage refers to the distance from the given landmark to the anterior margin of the tibia measured as a percentage of the maximum sagittal diameter of the tibia (line SD)

AM anteromedial, *PL* posterolateral

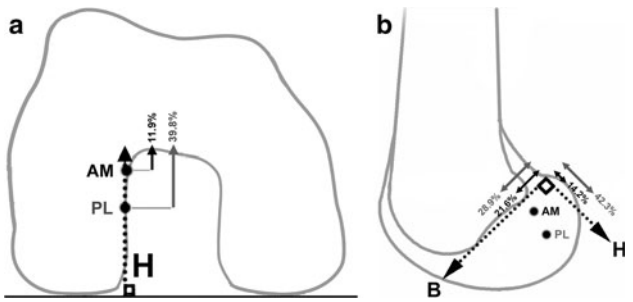

Fig. 4 Illustrations of a right femur in the AP (**a**) and lateral (**b**) radiographic views. Radiographic landmarks shown are qualitative representations and may not correspond quantitatively with the average positions reported in this study. Measurements are reported both in millimeters and as percentages of reference lines

between the femoral attachments centers of the AM and PL bundles was 8.6 mm. At 55° and 90° of knee flexion, these values were 8.8 mm and 5.6 mm, respectively. The AM bundle center was located 11.9% of the way down the maximum height of the intercondylar notch (line H), with respect to the notch roof, at 55° of flexion (88.1% from the bottom of the notch), whereas the position of the PL bundle center was 39.8% distal to the notch roof. At 90° of knee flexion, the AM bundle center was located at 18.4% and the PL bundle center at 39.1% of the maximum height of the intercondylar notch relative to the notch roof.

Lateral view

Radiographic measurements for the lateral view of the femur are illustrated in Fig. 4b and reported in Table 2. The distance between the attachment centers of the AM and PL bundles was 9.6 mm in the proximal–distal direction and 4.7 mm in the anterior–posterior direction. Analysis of the femoral attachments of the ACL bundles according to a previously described quadrant method [4, 6] revealed that distance B_p (the percent of the distance along Blumensaat's line) for the center of the AM bundle was 21.6% of line B and distance H_p (the percent distance along the maximum notch height) was 14.6% of line H. For the center of the PL bundle, distance B_p was 28.9% of line B, and distance H_p was 42.3% of line H. The knee flexion angle at which the AM and PL bundle attachment sites were oriented horizontally with respect to one another was 115°.

Tibia

Anterior–posterior view

Radiographic measurements for the AP view of the tibia are illustrated in Fig. 5a and reported in Table 3. The lateral–medial distance between the AM and PL bundle centers, measured parallel to the maximum coronal diameter of the tibia (line CD), was 5.7 mm. The center of the AM bundle was 44.2% from the medial aspect of the tibia along line CD, while the position of the PL bundle center was 50.1% of line CD.

Lateral view

Radiographic measurements for the lateral view of the tibia are illustrated in Fig. 5b and reported in Table 4. The anterior–posterior distance between the tibial attachment centers of the AM and PL bundles, measured parallel to the maximum sagittal diameter of the tibia (line SD), was 8.7 mm. The percentage-based locations of anatomic structures of interest from the anterior tibial margin along the maximum sagittal diameter of the tibia were as follows: the anterior edge of the AM bundle was 28.9%, the center of the AM bundle was 36.3%, the posterior edge of the AM bundle was 49.7%, the anterior edge of the PL bundle was 41.2%, the center of the PL bundle was 51.0%, and the posterior edge of the PL bundle was 59.3%.

Axial view

Radiographic measurements for the axial view of the tibia are illustrated in Fig. 5c and reported in Table 5. The center of the AM bundle was 48.0% along the maximum

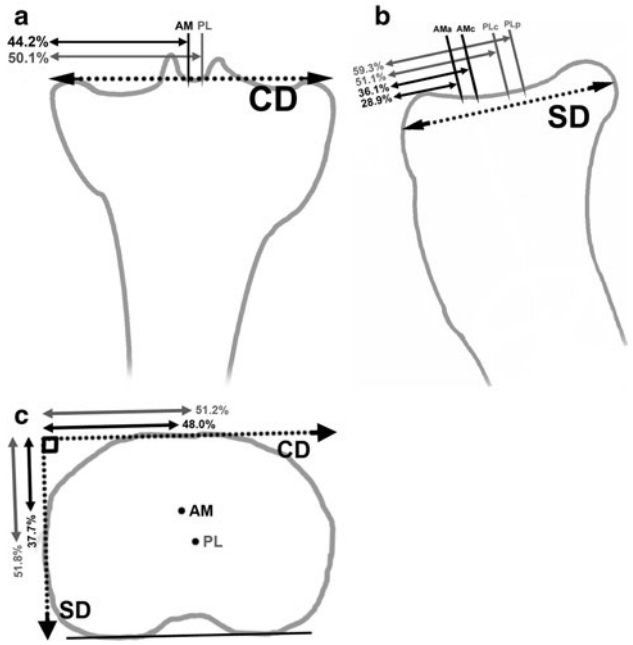

Fig. 5 Illustrations of a tibia in the AP (**a**), lateral (**b**), and axial (**c**) radiographic views. Radiographic landmarks shown are qualitative representations and may not correspond quantitatively with the average positions reported in this study. Measurements are reported both in millimeters and as percentage lengths along reference lines

coronal diameter of the axial section with respect to the medial tibial margin and 37.7% in reference to the anterior edge of the tibia along the maximum sagittal diameter, while the PL bundle was located at 51.2% with respect to the medial tibial margin along the coronal diameter and 51.8% in reference to the anterior edge of the tibia along the sagittal diameter.

Statistical analysis

Intraobserver ICCs were 0.989, 0.993, and 0.989 for examiners 1, 2, and 3, respectively, and the overall combined intraobserver ICC was 0.991. Interobserver reliability was assessed among the examiners in trial 1, trial 2, and with both trials combined. There was no significant difference between examiners for either trial state. The combined ICC for interobserver reliability was 0.990.

Discussion

The most important findings of this study in reference to the ACL bundle attachments on the femur were that the AM bundle attachment center was nearly adjacent to the roof of the intercondylar notch at approximately 10% of the maximum notch height measured with respect to the notch roof (90% with respect to the bottom of the notch), while the PL bundle attachment center was positioned 40% distal to the roof of the notch (60% proximal to the notch bottom); these values were consistent whether obtained on the AP femoral view with the knee flexed to 55°, or with application of the quadrant method [3] to the lateral view. In addition, the knee flexion angle at which the femoral attachment centers of the AM and PL bundles were oriented in the horizontal plane was 115°; temporarily flexing the knee to this angle during double-bundle ACL reconstructions could help establish a more distinct spatial relationship between the bundle centers and thus improve the ease and accuracy of femoral tunnel placement.

The most important findings regarding the ACL tibial bundle attachments were that the PL bundle attachment center was located almost precisely at the center of the tibia in both the coronal and sagittal radiographic views and thus can serve as a valuable reference for intra-operative tunnel positioning in fluoroscopic surgeries. Images of the tibia in the axial view provided further radiographic verification of the anterior-to-posterior and lateral-to-medial positions of the AM and PL bundle attachments as well as other landmarks for double-bundle ACL reconstruction. Measurements performed in this view not only further confirmed quantitative results gathered from AP to lateral knee radiographs, but could also be utilized in the analysis of axial MRI scans to assess tibial tunnel placement postoperatively.

A recent systemic literature review suggested that quantitative evaluations of the size and extent of ACL bundles footprints generally fail to yield consistent data or reliable clinical applications [11]. Nonetheless, certain qualitative similarities in femoral and tibial footprint morphology were observed radiographically among specimens in this study. In full extension, the femoral AM and PL bundle attachments were directly adjacent to and defined posteriorly by the posterior articular cartilage margin, with the superior extent of the AM bundle often approaching the most posterior aspect of the intercondylar notch roof and the PL bundle located farther distal and posterior on the lateral aspect of the intercondylar notch. Both bundles were approximately of similar size and oval in shape. In all specimens, the orientation between the tibial footprints of the AM and PL bundles was oblique, coursing posteromedial to anterolateral (Fig. 6). Previous descriptions of the tibial attachments have varied extensively: the relative orientation of the AM and PL bundle footprints has been characterized as strictly anterior–posterior [5, 12], medial–lateral [5, 18], and oblique, with the division between the bundles running posteromedial to anterolateral [11, 17]. The consistency of ACL tibial footprint morphology found in this study can be attributed to the method of carefully separating the ACL at the well-defined femoral ACL attachment sites with the specimens

flexed to >90°, allowing the distinct orientation and tensioning pattern of the fibers of each bundle to be more easily defined at its tibial attachment.

The use of intra-operative fluoroscopy and mechanically assisted navigation during double-bundle ACL reconstructions has become more common to enhance the accuracy of tunnel placement and reducing qualitative "guesswork" associated with these procedures. Shafizadeh et al. [16] reported combining fluoroscopic images of cadaveric knees with computerized, intra-operative acquisition of surface landmarks on the femur and tibia, which was used to plan and execute more precise femoral and tibial tunnel placement for single-bundle ACL reconstructions. Other studies have reported the successful application of three-dimensional navigation systems involving robotics, computer technology, and various mechanical apparatus to establish appropriate tunnel position in ACL reconstructions [20, 23]. The proposed radiographic guidelines could be utilized to rigorously assess both femoral and tibial tunnel positioning in three dimensions during double-bundle ACL reconstructions incorporating intra-operative fluoroscopy and a broad array of emerging navigational techniques. Furthermore, the present study incorporates soft-tissue and obscure osseous landmarks that are not readily visible on post-operative radiographs but which might be applicable in an intra-operative setting where computerized identification of these landmarks could be correlated with fluoroscopic images.

Certain limitations of the present study are acknowledged. While measurements in this study were performed on a relatively small number of cadaveric specimens, the size of these specimens was normalized according to the femoral epicondylar width. In addition, while the radiographic locations of anatomic landmarks were clearly labeled with radio-opaque markers in this study, we acknowledge that post-operative visualization of graft tunnels and intra-articular tunnel placement is generally difficult, especially considering that current double-bundle ACL reconstruction procedures often utilize cortical graft fixation on the femur and bioabsorbable screw fixation on the tibia.

Conclusions

In conclusion, this study defines the radiographic locations of the femoral and tibial bundle attachment sites of the native ACL and a reliable and transferrable protocol for identifying these sites on radiographs in relation to surrounding landmarks and digitally projected reference lines. In addition, it was found that the femoral attachments of the AM and PL bundles were horizontally aligned at 115° of knee flexion and the PL bundle tibial attachment was located essentially at the center of the tibia. These methods may be used to facilitate more accurate tunnel placement and to evaluate the positions of these tunnels both pre-operatively (in revision surgeries) and post-operatively in double-bundle ACL reconstructions.

Acknowledgments A grant from Health South-East Norway (grant #2009064) was used to pay for salaries of laboratory personnel, overhead expenses, supplies, illustrations, cadaveric knees, travel costs for researchers from the University of Oslo, and other expenses related to the study. The Minnesota Medical Foundation also awarded Medical Student Summer Research Grants to three authors (SDP, CGZ, CJA). The assistance of Conrad Lindquist and Paul Lender is acknowledged.

References

1. Aglietti P, Giron F, Cuomo P, Losco M, Mondanelli N (2007) Single-and double-incision double-bundle ACL reconstruction. Clin Orthop Relat Res 454:108–113
2. Amis AA, Jakob RP (1998) Anterior cruciate ligament graft positioning, tensioning and twisting. Knee Surg Sports Traumatol Arthrosc 6(Suppl 1):S2–S12
3. Bernard M, Hertel P, Hornung H, Cierpinski T (1997) Femoral insertion of the ACL. Radiographic quadrant method. Am J Knee Surg 10:14–21; discussion 21–22
4. Biau DJ, Tournoux C, Katsahian S, Schranz P, Nizard R (2007) ACL reconstruction: a meta-analysis of functional scores. Clin Orthop Relat Res 458:180–187
5. Colombet P, Robinson J, Christel P, Franceschi JP, Djian P, Bellier G, Sbihi A (2006) Morphology of anterior cruciate ligament attachments for anatomic reconstruction: a cadaveric dissection and radiographic study. Arthroscopy 22:984–992
6. Doi M, Takahashi M, Abe M, Suzuki D, Nagano A (2009) Lateral radiographic study of the tibial sagittal insertions of the anteromedial and posterolateral bundles of human anterior cruciate ligament. Knee Surg Sports Traumatol Arthrosc 17:347–351
7. Fithian DC, Paxton EW, Stone ML, Luetzow WF, Csintalan RP, Phelan D, Daniel DM (2005) Prospective trial of a treatment algorithm for the management of the anterior cruciate ligament-injured knee. Am J Sports Med 33:335–346
8. Freedman KB, D'Amato MJ, Nedeff DD, Kaz A, Bach BR Jr (2003) Arthroscopic anterior cruciate ligament reconstruction: a metaanalysis comparing patellar tendon and hamstring tendon autografts. Am J Sports Med 31:2–11
9. Gabriel MT, Wong EK, Woo SL, Yagi M, Debski RE (2004) Distribution of in situ forces in the anterior cruciate ligament in response to rotatory loads. J Orthop Res 22:85–89
10. Jarvela T (2007) Double-bundle versus single-bundle anterior cruciate ligament reconstruction: a prospective, randomize clinical study. Knee Surg Sports Traumatol Arthrosc 15:500–507
11. Kopf S, Musahl V, Tashman S, Szczodry M, Shen W, Fu FH (2009) A systematic review of the femoral origin and tibial insertion morphology of the ACL. Knee Surg Sports Traumatol Arthrosc 17:213–219
12. Luites JW, Wymenga AB, Blankevoort L, Kooloos JG (2007) Description of the attachment geometry of the anteromedial and posterolateral bundles of the ACL from arthroscopic perspective for anatomical tunnel placement. Knee Surg Sports Traumatol Arthrosc 15:1422–1431
13. Petersen W, Tretow H, Weimann A, Herbort M, Fu FH, Raschke M, Zantop T (2007) Biomechanical evaluation of two techniques for double-bundle anterior cruciate ligament reconstruction: one

tibial tunnel versus two tibial tunnels. Am J Sports Med 35:228–234
14. Pietrini SD, LaPrade RF, Griffith CJ, Wijdicks CA, Ziegler CG (2009) Radiographic identification of the primary posterolateral knee structures. Am J Sports Med 37:542–551
15. Schottle PB, Schmeling A, Rosenstiel N, Weiler A (2007) Radiographic landmarks for femoral tunnel placement in medial patellofemoral ligament reconstruction. Am J Sports Med 35:801–804
16. Shafizadeh S, Huber H, Grote S, Hoeher J, Paffrath T, Tiling T et al (2005) Principles of fluoroscopic-based navigation in anterior cruciate ligament reconstruction. Oper Tech Orthop 15:70–75
17. Siebold R, Ellert T, Metz S, Metz J (2008) Tibial insertions of the anteromedial and posterolateral bundles of the anterior cruciate ligament: morphometry, arthroscopic landmarks, and orientation model for bone tunnel placement. Arthroscopy 24:154–161
18. Takahashi M, Doi M, Abe M, Suzuki D, Nagano A (2006) Anatomical study of the femoral and tibial insertions of the anteromedial and posterolateral bundles of human anterior cruciate ligament. Am J Sports Med 34:787–792
19. Tsai AG, Wijdicks CA, Walsh MP, LaPrade RF (2010) Comparative kinematic evaluation of all-inside single-bundle and double-bundle anterior cruciate ligament reconstruction: a biomechanical study. Am J Sports Med 38:263–272
20. Van de Velde SK, Gill TJ, Li G (2009) Evaluation of kinematics of anterior cruciate ligament-deficient knees with use of advanced imaging techniques, three-dimensional modeling techniques, and robotics. J Bone Joint Surg Am 91(Suppl 1):108–114
21. Walsh MP, Wijdicks CA, Parker JB, Hapa O, LaPrade RF (2009) A comparison between a retrograde interference screw, suture button, and combined fixation on the tibial side in an all-inside anterior cruciate ligament reconstruction: a biomechanical study in a porcine model. Am J Sports Med 37:160–167
22. Wijdicks CA, Griffith CJ, LaPrade RF, Johansen S, Sunderland A, Arendt EA, Engebretsen L (2009) Radiographic identification of the primary medial knee structures. J Bone Joint Surg Am 91:521–529
23. Woo SL, Fisher MB (2009) Evaluation of knee stability with use of a robotic system. J Bone Joint Surg Am 91(Suppl 1):78–84
24. Yagi M, Wong EK, Kanamori A, Debski RE, Fu FH, Woo SL (2002) Biomechanical analysis of an anatomic anterior cruciate ligament reconstruction. Am J Sports Med 30:660–666
25. Zantop T, Kubo S, Petersen W, Musahl V, Fu FH (2007) Current techniques in anatomic anterior cruciate ligament reconstruction. Arthroscopy 23:938–947
26. Zantop T, Wellmann M, Fu FH, Petersen W (2008) Tunnel positioning of anteromedial and posterolateral bundles in anatomic anterior cruciate ligament reconstruction: anatomic and radiographic findings. Am J Sports Med 36:65–72